

Water table fluctuations affect dichloromethane biodegradation in lab-scale aquifers contaminated with organohalides

Maria Prieto-Espinoza^a, Sylvain Weill^a, Benjamin Belfort^a, Emilie E.L. Muller^b,
Jérémy Masbou^a, François Lehmann^a, Stéphane Vuilleumier^b, Gwenaél Imfeld^{a,*}

^a Université de Strasbourg, CNRS/EOST, ITES UMR 7063, Institut Terre et Environnement de Strasbourg, Strasbourg, France

^b Université de Strasbourg, CNRS, GMGM UMR 7156, Génétique Moléculaire, Génomique, Microbiologie, Strasbourg, France

ARTICLE INFO

Keywords:

DCM degradation
Laboratory Aquifers
Dynamic conditions
Multi-element CSIA, 16s rRNA

ABSTRACT

Dichloromethane (DCM) is a toxic industrial solvent frequently detected in multi-contaminated aquifers. It can be degraded biotically or abiotically, and under oxic or anoxic conditions. The extent and pathways of DCM degradation in aquifers may thus depend on water table fluctuations and microbial responses to hydrochemical variations. Here, we examined the effect of water table fluctuations on DCM biodegradation in two laboratory aquifers fed with O₂-depleted DCM-spiked groundwater from a well-characterized former industrial site. Hydrochemistry, stable isotopes of DCM ($\delta^{13}\text{C}$ and $\delta^{37}\text{Cl}$), and bacterial community composition were examined to determine DCM mass removal and degradation pathways under steady-state (static water table) and transient (fluctuating water table) conditions. DCM mass removal was more pronounced under transient (95%) than under steady-state conditions (42%). C and Cl isotopic fractionation values were larger under steady-state ($\epsilon_{\text{bulk}}^{\text{C}} = -23.6 \pm 3.2\text{‰}$, and $\epsilon_{\text{bulk}}^{\text{Cl}} = -8.7 \pm 1.6\text{‰}$) than under transient conditions ($\epsilon_{\text{bulk}}^{\text{C}} = -11.8 \pm 2.0\text{‰}$, and $\epsilon_{\text{bulk}}^{\text{Cl}} = -3.1 \pm 0.6\text{‰}$). Dual C-Cl isotope analysis suggested the prevalence of distinct anaerobic DCM degradation pathways, with $\Delta^{\text{C/Cl}}$ values of 1.92 ± 0.30 and 3.58 ± 0.42 under steady-state and transient conditions, respectively. Water table fluctuations caused changes in redox conditions and oxygen levels, resulting in a higher relative abundance of *Desulfosporosinus* (*Peptococcaceae* family). Taken together, our results show that water table fluctuations enhanced DCM biodegradation, and correlated with bacterial taxa associated with anaerobic DCM degradation. Our integrative approach allows to evaluate anaerobic DCM degradation under dynamic hydrogeological conditions, and may help improving bioremediation strategies at DCM contaminated sites.

1. Introduction

Dichloromethane (DCM, CH₂Cl₂) is a toxic, persistent and halogenated volatile organic compound (VOC) widely used in industrial settings (Schlosser et al., 2015). Due to accidental spills and improper storage at industrial sites, DCM is commonly detected in contaminated aquifers along with other VOCs (EPA, 2020; Hermon et al., 2018; Shestakova & Sillanpää, 2013). DCM is included in the list of priority pollutants of the U.S. Agency for Toxic Substances and Disease Registry (ATSDR, 2019), and of the European Commission (European Commission, 2013).

Monitored natural attenuation (MNA) has become a promising remediation strategy to detoxify contaminated aquifers (Pope et al., 2004; Smets & Pritchard, 2003). MNA relies on an integrative approach,

which includes (i) monitoring contaminant concentrations in the field, (ii) laboratory assays with microorganisms from the field, and (iii) evidence of *in situ* biodegradation potential using stable isotope analysis and/or biomolecular methods (NRC, 1993). Monitoring contaminant concentrations is not sufficient to identify contaminant transformation, as concentrations alone reflect both non-destructive (e.g., dilution, sorption) and destructive dissipation processes (e.g., biodegradation). Compound-specific isotope analysis (CSIA) is increasingly used to measure the extent of contaminant transformation *in situ* (Hunkeler et al., 2009). CSIA relies on changes in stable isotope ratios (e.g., ¹³C/¹²C) of an organic contaminant undergoing a (bio)degradation reaction. Typically, molecules containing light isotopes (e.g., ¹²C) are degraded preferentially compared to those containing heavy isotopes (e.g., ¹³C). This generally results in a change of stable isotope ratios in the

* Corresponding author.

E-mail address: imfeld@unistra.fr (G. Imfeld).

<https://doi.org/10.1016/j.watres.2021.117530>

Received 3 March 2021; Received in revised form 28 July 2021; Accepted 2 August 2021

Available online 6 August 2021

0043-1354/© 2021 Elsevier Ltd. All rights reserved.

remaining contaminant mass, which may be specific of the transformation pathway (Elsner and Imfeld, 2016). The stable isotope fractionation can be used for quantitative estimations of contaminant transformation *in situ* by using isotope fractionation values (ϵ) derived from reference laboratory experiments (Fischer et al., 2016).

Dual-isotope analysis, involving the follow-up of changes in isotope ratios of two elements (e.g., $^{13}\text{C}/^{12}\text{C}$ and $^{37}\text{Cl}/^{35}\text{Cl}$), is more informative and robust than a single isotope element approach to evaluate transformation pathways of organic contaminants (Ojeda et al., 2020). When stable isotope ratios of two elements are compared in a dual plot, the slope (Λ) provides a quantitative parameter of the corresponding transformation pathway (Elsner, 2010; Ojeda et al., 2020). For DCM, the transformation pathway of methylotrophic bacteria, featuring a glutathione-dependent DCM dehalogenase, was the first to be examined by dual C-Cl CSIA under oxic conditions ($^{13}\text{C}/^{12}\text{C}$ and $^{37}\text{Cl}/^{35}\text{Cl}$) (Heraty et al., 1999; Torgonskaya et al., 2019). Recently, dual C-Cl CSIA provided evidence of distinct anaerobic DCM pathways for *Dehalobacterium formicoaceticum*, and for mixed cultures containing DCM-degrading organisms such as *Candidatus Dichloromethanomonas elyunquensis* (Chen et al., 2018; Kleindienst et al., 2019), and for a bacterial consortium featuring a *Dehalobacterium* strain (Blázquez-Pallí et al., 2019; Truaba-Santiso et al., 2017).

So far, DCM transformation pathways have been examined in groundwater microcosms under static conditions. However, the interplay of hydrochemical and hydrogeological dynamics in DCM biodegradation in contaminated aquifers has not yet been addressed. Water table fluctuations are known to affect (i) mass transfer of VOCs (e.g., DCM) from groundwater to the unsaturated zone (Jeannot and Hunkeler, 2013; McCarthy and Johnson, 1993), (ii) redox conditions due to redistribution of terminal electron acceptors (e.g., O_2) (Haberer et al., 2012; Seybold et al., 2002), and (iii) bacterial community composition due to changes in nutrients, redox conditions and exposure to pollutants (Peralta et al., 2014; Rühle et al., 2015). The effect of water table fluctuations on DCM biodegradation is difficult to probe *in situ* as it requires a high spatial and temporal monitoring resolution (Zhang and Furman, 2021). In this context, laboratory aquifers under near-natural settings may prove useful, as flow fields can be controlled and mass fluxes can be established (Schürner et al., 2016).

The purpose of the present study was to examine the effect of water table fluctuations on hydrochemistry, bacterial community composition, and DCM degradation extent and pathways under controlled conditions. Two laboratory aquifers, fed with contaminated groundwater from a well-characterized former industrial site (Hellal et al., 2021; Hermon et al., 2018), were set up to examine the reactive transport of DCM under transient (i.e., induced water table fluctuations) and steady-state (i.e., static water table) conditions. Concentrations of chloroethenes *cis*-DCE and VC in the contaminated groundwater were also monitored. The objectives of the present study were (i) to examine DCM dissipation processes in groundwater under steady-state and transient conditions, (ii) to infer DCM degradation pathways using dual C-Cl CSIA, and (iii) to analyse bacterial community composition associated with DCM biodegradation by sequencing the 16S rRNA gene.

2. Materials and methods

2.1. Chemicals

DCM, *cis*-DCE and VC standards were purchased from Sigma-Aldrich (St. Louis, MO, USA; analytical grade purity: >99%). A second DCM standard was purchased from VWR (Radnor, Pennsylvania, USA; analytical grade purity: >99%). Stock solutions of standards were prepared in methanol at 1 g L^{-1} and diluted in water. Aliquots were stored at 4°C . DCM standards from Sigma-Aldrich and VWR are referenced here as DCM_{#1} and DCM_{#2}, respectively.

2.2. Groundwater

Groundwater was collected from the source zone of a well-characterized contaminated aquifer (well Pz-28; Hellal et al., 2021; Hermon et al., 2018), and used as inflow water in both laboratory aquifers. Isotope and biomolecular analyses evidenced *in situ* anaerobic DCM and *cis*-DCE biodegradation in the source zone of the contaminated aquifer, as well as bacterial genera associated with organohalide respiration (OHR) such as *Geobacter* and *Dehalococcoides* (Hellal et al., 2021; Hermon et al., 2018). Field groundwater sampling and hydrochemical characteristics are provided as Supporting Information (SI, Sections A and F).

2.3. Experimental setup

Experiments were conducted in two laboratory aquifers with inner dimensions of $160\text{ cm} \times 80\text{ cm} \times 7\text{ cm}$ (length \times height \times width) and filled with sterile quartz sand (grain size: $0.4 - 0.6\text{ mm}$; depth: 70 cm). A headspace zone of 10 cm above the sand compartments was covered by a top glass mounted with 3 sampling ports equipped with active charcoal cartridges and opened to the atmosphere (Fig. 1). A detailed description of the experimental setup is provided in SI (Section B). Experiments were conducted in a temperature-controlled room at $18 \pm 1^\circ\text{C}$. Both aquifers were continuously fed with O_2 -depleted contaminated groundwater ($\text{O}_2 < 1\text{ mg L}^{-1}$) at a rate of 430 mL d^{-1} , corresponding to an average water velocity of 0.02 m d^{-1} . Groundwater was supplied from two sterile and gas-tight 10 L glass reservoirs connected to each aquifer (Fig. 1). Each reservoir was kept under constant N_2 -flux and consisted of a mixture of groundwater and sterilized O_2 -depleted distilled water at a ratio of 1:3. This allowed to avoid clogging of the pipes feeding the aquifers due to mineral precipitation. Pure DCM was directly spiked and mixed into the reservoirs to reach aqueous concentrations of 0.47 mM L^{-1} , equivalent to typical concentrations at contaminated sites (Hermon et al., 2018; Wright et al., 2017).

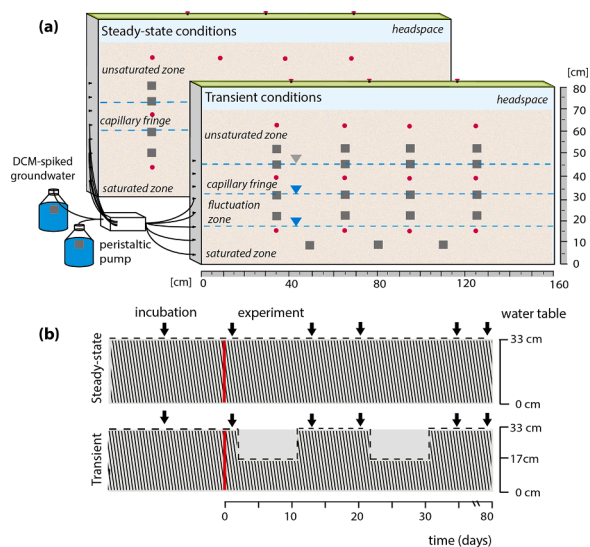


Fig. 1. Lab-scale aquifers fed with DCM-spiked groundwater under steady-state and transient conditions. (a) Schematic overview of the aquifers (flow path from left to right) indicating the saturated zone (SZ), unsaturated zone (UZ), headspace, position of sampling ports (red dots), oxygen foils (grey squares) and top glass (green) covering the aquifers along with three sampling ports opened to the atmosphere. (b) Operations to establish steady-state and transient conditions in the laboratory aquifers and sampling. Water table level is indicated in dotted lines. The end of the incubation period (total 70 days) is marked with a red line. Black arrows show sampling events of water and gas samples. Sampling within the incubation period took place 35 days prior to the experiment.

2.4. Laboratory aquifer operations

Both aquifers were operated simultaneously. Prior to the experiments, an incubation period of 70 days was established by operating both aquifers with a continuous flow of DCM-spiked groundwater to reach initial steady-state conditions and allow bacterial adaptation. Monitoring of DCM concentrations and carbon stable isotope ratios during the incubation period (70 days) evidenced DCM biodegradation capacity in both aquifers (data not shown). The water table was positioned at a depth of 33 cm and a capillary fringe of approximately 12 cm was determined visually. During the experimental phase (day 0 to 88), one aquifer remained under steady-state conditions while the second aquifer underwent two water table fluctuation events (Fig. 1). Under steady-state conditions, a constant horizontal water flow was established using a peristaltic pump (IPC 8, ISMATEC, Glattbrugg, Switzerland). Transient conditions were established by (i) lowering the water table by 16 cm for 24 h (day 3), (ii) continuous horizontal flow at a low water level for 6 d (up to day 10), and (iii) raising the water table to its initial position for 24 h (day 11). A second identical water table fluctuation event was performed from day 21 to 32 (Fig. 1).

2.5. Sampling

Sampling was carried out in both aquifers before and after each water table fluctuation event on days 0 and 13 (first water table fluctuation), and at days 20 and 35 (second water table fluctuation). Pore water samples were collected for hydrochemical analysis, VOCs concentration measurements, carbon and chlorine isotope analysis, and bacterial diversity and community composition. Pore water samples were collected using gas-tight syringes (Hamilton Bonaduz AG, Bonaduz, Switzerland) from inlet and outlet reservoirs, and sampling ports located at depths of 15 and 40 cm from the bottom, and at 35, 65, 95 and 125 cm from the inflow (Fig. 1). For quantification and CSIA, 20 mL glass vials (Interchim, Montluçon, France) were filled with 1 mL of pore water sample and 1 mL of saturated salt solution (triplicate measurements). Vials were immediately crimped with a Teflon septum with a magnetic crimp (Interchim, Montluçon, France), and stored upside down at 4°C until further analysis. Gas-phase samples (volume: 2 cm³) were collected from the unsaturated zone ($z = 65$ cm) and headspace ($z = 80$ cm), and stored similarly as liquid samples.

Water samples for DNA analysis were collected from inlet and outlet reservoirs (8 mL) and from sampling ports located at depths of 15 and 40 cm (pooling 2 mL in total per single height). Additionally, pore water samples were collected during the incubation period (35 days prior to the experiments, see Fig. 1), and prior to the core sampling (day 80) for DNA and hydrochemical analysis. At the end of the experiment, both aquifers were fully drained and sand samples from four cores (length: 70 cm, and inner diameter: 5 cm) were collected for DNA analysis into sterile polyethylene tubes, and stored at -20 °C until further analysis. Core sand samples covering the full depth of the aquifers were retrieved at 40, 70, 100, and 130 cm from the inflow. Three core subsamples representing the saturated zone (SZ), capillary fringe (CF) and unsaturated zones (UZ) were obtained by cutting under sterile conditions each frozen sand core at depths of 25 and 50 cm, respectively.

2.6. Analytical methods

2.6.1. Hydrochemistry

Oxygen (O₂) concentrations were monitored *in situ* by O₂ sensitive optode foils (PreSens GmbH, Regensburg, Germany) located at the inlet reservoirs and across the sand compartments (Fig. 1). Under transient conditions, O₂ concentrations were monitored hourly during water table fluctuation events. Redox potential (Eh), pH and electrical conductivity were monitored prior to sampling events using laboratory probes (SCHOTT® Instruments). Major ions were measured by ion chromatography (Dionex ICS-5000, Thermo Scientific, USA). Fe²⁺ was

measured by the BAP method (Tamura et al., 1974). Total organic carbon (TOC), dissolved organic carbon (DOC) and dissolved inorganic carbon (DIC) were analyzed by a TOC analyzer (TOC-V-CPH Shimadzu, NF EN 1484).

2.6.2. VOCs concentrations and DCM C-Cl CSIA analysis

A detailed description of analytical methods is given in the SI (Sections C and D). Briefly, DCM, *cis*-DCE and VC were quantified by analyzing 200 µL of headspace sample using a gas chromatograph (GC, Trace 1300, Thermo Fisher Scientific) coupled with a mass spectrometer (MS, ISQ™, Thermo Fisher Scientific), as described elsewhere (Hermon et al., 2018).

Stable carbon isotope composition of DCM, *cis*-DCE and VC was determined by gas chromatography-combustion-isotope ratio mass spectrometry (GC-C-IRMS), with a gas chromatograph (Trace 1310) coupled via a GC/Conflow IV interface to an isotope ratio mass spectrometer (Delta V plus, Thermo Fisher Scientific) (Hermon et al., 2018). In-house standards of DCM, *cis*-DCE and VC were prepared daily and analyzed prior to sample measurements. Reproducibility of triplicate measurements was ≤0.2‰ (1σ) within the linearity range (0.5-50 mg L⁻¹). Carbon isotope ratios were reported in δ notation as parts per thousand (‰) relative to the international reference material Vienna Pee Dee-Belemnite (V-PDB) (Coplen et al., 2006).

Chlorine isotope composition of DCM was determined by GC-qMS based on the two most abundant fragment ion peaks [³⁵Cl¹²C₁H₂]⁺ (m/z 49) and [³⁷Cl¹²C₁H₂]⁺ (m/z 51), as suggested elsewhere (Heckel et al., 2017; Jin et al., 2011). The detailed GC-qMS setup is provided as SI (Section D). Chlorine isotope ratios were reported in δ notation in parts per thousand [‰] relative to the Standard Mean Ocean (SMOC) (Kaufmann et al., 1984). Chlorine isotope ratios were corrected by an external two-point calibration with pure DCM in-house standards ($\delta^{37}\text{Cl}_{\text{DCM}\#1} = 3.68 \pm 0.10\%$ and $\delta^{37}\text{Cl}_{\text{DCM}\#2} = -3.35 \pm 0.12\%$) characterized at Isotope Tracer Technologies Inc., Waterloo, Canada by IRMS after conversion to CH₃Cl (Holt et al., 1997), and at the Departament de Mineralogia, Petrologia i Geologia Aplicada, University of Barcelona using GC-qMS. Reported uncertainties include both accuracy and reproducibility based on long-term measurements and standard deviations. Typical reproducibility was 0.5‰ (1σ) within the tested linearity range (0.5-20 mg L⁻¹). Chlorine isotope compositions of native *cis*-DCE and VC were not analyzed.

2.6.3. DNA extraction from pore water and sand samples

Pore water samples were filtered through sterile 0.22 µm membrane filters (Swinnex holder, 13 mm, Millipore, Bedford, USA) and stored at -20°C until DNA extraction, as described previously (Hermon et al., 2018). Sand core subsamples were retrieved from both aquifers at the end of the experiments (day 88). Under sterile conditions, the bottom and top first 1 cm of the core samples were removed. Each core subsample was thoroughly mixed and a representative subsample of 1 g of sand was used for DNA extraction. For both pore water and core samples, DNA was extracted using the DNeasy Power Water kit according to the manufacturer's protocol (Qiagen, Hilden, Germany). Extracted DNA was quantified using Qubit fluorometric quantification with the Qubit dsDNA HS Assay kit (ThermoFischer Scientific, MA, USA)

2.6.4. DNA sequencing

The V4-V5 hypervariable region of the 16S rRNA gene was PCR amplified by an optimized and standardized amplicon library preparation protocol (Metabiotec®, GenoScreen, Lille, France), including positive (mock community) and negative (blank) controls (Hermon et al., 2018). Libraries were sequenced by paired-end Illumina MiSeq 2 × 250 bases. Demultiplexing and trimming was followed by paired read assembly (minimum overlap 30 nt, minimum identity of 97%), resulting in a total of 3,614,309 sequences. Denoising, chimera checking, generation of operational taxonomic units (OTUs), taxonomic classification using Greengenes (v13.8 as reference), and alpha-diversity metrics were

performed using a custom-scripted bioinformatics pipeline of Genoscreen (Hermon et al., 2018). The percentage of 16S rRNA gene sequences of taxa featuring known DCM-degrading strains (identity >97%) was determined.

2.7. Data analysis

2.7.1. Evaluation of isotopic data

The average isotope value of the residual non-degraded fraction of DCM was derived according to the Rayleigh equation (Elsner, 2010):

$$\ln\left(\frac{R_{t,E}}{R_{0,E}}\right) = \ln\left(\frac{C_{t,E}}{C_{0,E}}\right) \cdot \frac{\epsilon_{bulk}^E}{1000} \quad (1)$$

where $R_{t,E}/R_{0,E}$ is the isotope ratio of element “E” (i.e., $^{13}\text{C}/^{12}\text{C}$ and $^{37}\text{Cl}/^{35}\text{Cl}$) and $C_{t,E}/C_{0,E}$ are the concentrations at a given time (t) and at the initial time (0). Carbon and chlorine isotopic composition were reported in delta notation ($\delta^h\text{E}$) following $\delta^h\text{E} = [(R_{\text{sample}}/R_{\text{standard}}) - 1] \times 1000$ (Elsner, 2010). Apparent isotope fractionation values (ϵ_{bulk}^E , in ‰) were obtained by least squares linear regression without forcing the slope through the origin. The uncertainty corresponds to the 95% confidence interval (C.I.) and the error was determined using ordinary linear regression (Elsner et al., 2007).

Changes of carbon versus chlorine isotope signatures were plotted to derive the $\Lambda^{C/Cl}$ value from the slope of the linear regression using the least-squares algorithm of the York method (Höhener and Imfeld, 2021; Ojeda et al., 2020), and using the IsoplotR package in R (Vermeesch, 2018). (Eqs. 2)

$$\Lambda^{C/Cl} = \frac{\ln[(\delta^{13}\text{C}_t/1000 + 1)/(\delta^{13}\text{C}_0/1000 + 1)]}{\ln[(\delta^{37}\text{Cl}_t/1000 + 1)/(\delta^{37}\text{Cl}_0/1000 + 1)]} \approx \frac{\epsilon_{bulk}^C}{\epsilon_{bulk}^{Cl}} \quad (2)$$

DCM biodegradation was estimated based on changes in carbon and chlorine isotope ratios over time and across the flow path (i.e., at different observation points). The extent of DCM biodegradation (B , in %) was estimated using the Rayleigh model (Hunkeler et al., 2005; Thullner et al., 2012). A range of B was obtained from reported ϵ^C and ϵ^{Cl} values for both aerobic and anaerobic bacterial DCM degradation (Torgonskaya et al., 2019; Chen et al., 2018; Lee et al., 2015).

$$B (\%) = 1 - f = \left[\frac{\delta^h E_t + 1000}{\delta^h E_0 + 1000} \right]^{\frac{1000}{\epsilon^E}} \cdot 100 \quad (3)$$

2.7.2. Bacterial community composition

Sequencing data from pore water and sand samples were deposited to the ENA archive, BioProject accession number PRJEB43379. Multivariate statistical analysis of relative OTU abundance was performed with R (R Core Team, 2019). Non-metric multidimensional scaling (NMDS) based on Bray-Curtis dissimilarities of log-transformed data was performed to visualize dissimilarities between bacterial taxa associated with DCM degradation (Hellal et al., 2021).

3. Results and discussion

3.1. Water table fluctuations affect hydrochemical conditions

Hydrochemical variations are summarized in the SI (Sections E and F). Overall, saturated O_2 concentrations (8.4 mg L^{-1}) were observed in the unsaturated zone (UZ) in both aquifers ($z = 60 \text{ cm}$), while O_2 -depleted levels were established in the saturated zone (SZ; $z = 0\text{--}33 \text{ cm}$; $\text{O}_2 < 1.0 \text{ mg L}^{-1}$). The increase of redox potential over time (E_h ranged from -100 to $+0 \text{ mV}$ at days 0 and 35, respectively) was consistent with O_2 dynamics in the fluctuation zone ($z = 17\text{--}33 \text{ cm}$, SI Section F) (Pronk et al., 2020). Concentrations of O_2 rapidly increased up to 1.5 mg L^{-1} during drainage periods ($z = 25 \text{ cm}$, SI, Section E). During the first imbibition period, water moved in an upward direction, O_2 concentrations decreased slightly but did not return to initial concentrations (1.3

mg L^{-1}). From the second imbibition period until the end of the experiment, O_2 levels slowly decreased indicating that the system progressively returned to initial conditions ($\text{O}_2 < 1 \text{ mg L}^{-1}$) (Haberer et al., 2012). Re-oxygenation of groundwater below the water table was likely associated with entrapped air serving as a source of O_2 to the underlying O_2 -depleted water (Williams and Oostrom, 2000). Redox potential and O_2 varied upon water table fluctuation. Nevertheless, the high concentration of Fe^{2+} in both aquifers (up to 2.8 mg L^{-1}) suggested prevailing reducing conditions, in line with reducing conditions observed *in situ* for the groundwater used in this study (Hellal et al., 2021; Hermon et al., 2018) (SI, Section F). No other reduced species were detected in both aquifers ($< \text{D.L.}$).

Cis-DCE and VC, the two main chloroethenes in the groundwater source of this study (Hellal et al., 2021; Hermon et al., 2018), were also followed to further examine the established hydrochemical conditions in the laboratory aquifers. Only *cis*-DCE was detected at the inflow of both aquifers with average concentrations of 15 mg L^{-1} and $\delta^{13}\text{C}_{\text{DCE}}$ values of $-23.5 \pm 0.4\text{‰}$ (SI, Section G). Up to 90% of *cis*-DCE dissipated at the outflows after 35 days. Values of $\delta^{13}\text{C}$ for *cis*-DCE were smaller ($\Delta\delta^{13}\text{C}_{\text{DCE}} < 2\text{‰}$) at the outflows than $\delta^{13}\text{C}$ values observed within the first 65 cm from inflow ($\Delta\delta^{13}\text{C}_{\text{DCE}} > 10\text{‰}$). Similarly, VC concentrations of up to 6 and 12 mg L^{-1} were detected within the first 65 cm from inflow under steady-state and transient conditions, respectively, and average $\delta^{13}\text{C}_{\text{VC}}$ values of $-39.2 \pm 0.8\text{‰}$ ($n = 20$) were formed along the flow path ($\delta^{13}\text{C}_{\text{VC, standard}} = -29.5 \pm 0.2\text{‰}$) (SI, Section G). Together with the detection of OHRB (see below), this suggests that reductive dechlorination occurred in both aquifers, in agreement with observations at the groundwater source (Hellal et al., 2021, Hermon et al., 2018).

3.2. Water table fluctuations affect DCM mass dissipation and C and Cl isotope fractionation

The absence of gas-phase DCM (gas-phase Q.L. = $0.13 \mu\text{g L}^{-1}$, sampling volume: 2 cm^3) in the UZ ($z = 65 \text{ cm}$) and headspace ($z = 80 \text{ cm}$) of both aquifers throughout the experiment, and inlet-outlet DCM mass balance indicated that volatilization did not contribute significantly ($< 10\%$) to the overall DCM dissipation in both aquifers. Steep concentration gradients are generally formed across the capillary fringe due to slow diffusion in water and small vertical dispersivity (Jeannotat and Hunkeler, 2013). Previous studies showed that mass transport of PCE and TCE from the SZ to the UZ (i.e., within the 15 cm above the water table) led to 90% smaller gas-phase concentrations with respect to the aqueous-phase concentrations at the water table under steady-state (Jeannotat and Hunkeler, 2013, McCarthy and Johnson, 1993). While variations of VOCs concentrations in the gas-phase increase in the UZ when the water table drops as a result of residual water being in contact with the gas, concentrations decrease again when the water table is raised, returning to concentration equilibrium (Jeannotat and Hunkeler, 2013; McCarthy and Johnson, 1993). Hence, undetected gas-phase DCM concentrations in the UZ ($z = 65 \text{ cm}$) and headspace ($z = 80 \text{ cm}$) is likely due to (i) the low non-dimensional Henry's coefficient of DCM of 0.0549 at 18°C (Gossett, 1987; non-dimensional Henry's coefficient of PCE and TCE of 0.495 and 0.265, respectively), (ii) the continuous replenishment of the aqueous phase by horizontal groundwater flow, and (iii) measurements carried out under near-equilibrium conditions, before and after each water table fluctuation event.

In the SZ, DCM concentrations decreased along the flow path in both aquifers. After 35 days, a more pronounced DCM mass dissipation in the aquifer outlets was observed under transient (95%) than under steady-state (42%) conditions (Fig. 2). $\delta^{13}\text{C}$ and $\delta^{37}\text{Cl}$ values of DCM in the inflow water remained constant throughout the experiments ($-46.3 \pm 0.5\text{‰}$ and $-3.5 \pm 0.12\text{‰}$, respectively). Under both transient and steady-state conditions, DCM became significantly enriched in both ^{13}C and ^{37}Cl (Fig. 2). C and Cl isotope data for DCM degradation showed a good fit to the Rayleigh model (eq. 1) under both hydraulic regimes (R^2

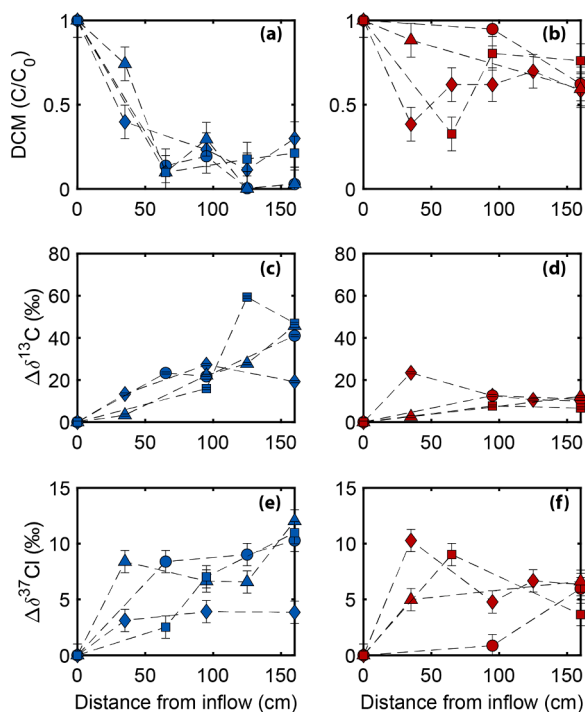


Fig. 2. DCM concentrations under steady-state (red) and transient (blue) conditions (a, b), carbon isotope values (c, d) and chlorine isotope values (e, f) over distance from inflow. Symbols represent observations at depth $z = 15$ cm and at different times: day 0 (diamonds), day 13 (circles), day 20 (triangles) and day 35 (squares). Error bars associated with DCM concentrations and stable isotope values represent standard errors ($3 \leq n$).

> 0.92) (SI, Section H). Apparent C and Cl isotope fractionation values ($\epsilon_{\text{bulk}}^{\text{C}}$ and $\epsilon_{\text{bulk}}^{\text{Cl}}$) of $-23.6 \pm 3.2\text{‰}$ and $-8.7 \pm 1.6\text{‰}$, respectively, were larger under steady-state than under transient conditions ($\epsilon_{\text{bulk}}^{\text{C}}$ and $\epsilon_{\text{bulk}}^{\text{Cl}}$ values of $-11.8 \pm 2.0\text{‰}$ and $-3.1 \pm 0.6\text{‰}$, respectively; SI, Section H). In previous reports, DCM volatilization was associated with low C and Cl fractionation ($\epsilon^{\text{C}} = +0.65\text{‰}$ and $\epsilon^{\text{Cl}} = -0.48\text{‰}$) compared to DCM biodegradation (Huang et al., 1999). Thus, the magnitude of $\epsilon_{\text{bulk}}^{\text{C}}$ and $\epsilon_{\text{bulk}}^{\text{Cl}}$ values under both hydraulic regimes suggest that DCM biodegradation prevailed in the aquifers.

The extent of DCM biodegradation (B) along the flow path was calculated based on reported ϵ^{C} values ranging from -71‰ to -15.5‰ and ϵ^{Cl} values from -7‰ to -5.2‰ (Torgonskaya et al., 2019, Chen et al., 2018, Lee et al., 2015). The range of ϵ^{C} and ϵ^{Cl} values was defined based on the assumption that both aerobic and anaerobic DCM degradation pathways co-occur in both aquifers, which is supported by hydrochemical variations and micro-oxic environments in the groundwater source (Hermon et al., 2018). Values of B under steady-state and transient conditions ranged from 22% to 55%, and from 22% to 90%, respectively (Table 1), corresponding to the DCM mass dissipation

Table 1

DCM biodegradation (B [%]) under transient and steady-state conditions from days 0 to 35. A range of B [%] was estimated using the full range of ϵ^{C} and ϵ^{Cl} values reported so far for both aerobic and anaerobic bacterial degradation of DCM. Reported values range from -27‰ (C_{Bmin}) to -15.5‰ (C_{Bmax}), and ϵ^{Cl} value of -7‰ (Cl_{Bmin}) to -5.2‰ (Cl_{Bmax}) (Torgonskaya et al., 2019, Chen et al., 2018, Lee et al., 2015).

Condition	Days	$\Delta\delta^{13}\text{C}$ [‰]	$\Delta\delta^{37}\text{Cl}$ [‰]	C_{Bmin} [%]	C_{Bmax} [%]	Cl_{Bmin} [%]	Cl_{Bmax} [%]
Transient	0	17.6	4.8	22	66	48	58
	13	31.8	9.2	36	85	73	83
	20	40.3	10.3	33	86	80	85
	35	49.2	7.0	48	91	66	75
	Steady-state	0	17.6	5.6	22	66	55
Steady-state	13	11.7	5.9	16	54	34	43
	20	12.1	5.8	14	48	56	67
	35	11.6	6.3	15	51	57	66

observed under both hydraulic regimes. Time-dependent first-order biodegradation rate constants (λ_t) were calculated according to the Rayleigh model, as described in the SI of Hermon et al., 2018, with values of $3.4 \times 10^{-3} \text{ d}^{-1}$ and $5.7 \times 10^{-3} \text{ d}^{-1}$ under steady-state and transient conditions, respectively. Worthy of note, similar *in situ* λ_t were estimated at the groundwater source of this study (Hermon et al. 2018), thus demonstrating the established near-natural settings within the laboratory aquifers.

3.3. DCM transformation pathways under transient and steady-state conditions

Estimated $\Lambda^{\text{C/Cl}}$ values were lower under steady-state (1.92 ± 0.30 , $p < 0.03$) than under transient conditions (3.58 ± 0.42 , $p < 0.01$) (Fig. 3). This suggests distinct DCM C-Cl bond cleavage mechanisms under dynamic hydrogeological conditions. The calculated $\Lambda^{\text{C/Cl}}$ values under transient conditions fall within the range of reported $\Lambda^{\text{C/Cl}}$ values during anaerobic DCM degradation (3.40-7.89) and are similar to $\Lambda^{\text{C/Cl}}$ values reported for *Ca. Dichloromethanomonas elyunquensis* (3.40 ± 0.03) (Chen et al., 2018), which suggests the prevalence of anaerobic DCM pathways. Most strikingly, the lower $\Lambda^{\text{C/Cl}}$ value determined under steady-state conditions (1.92 ± 0.30) has not been reported previously.

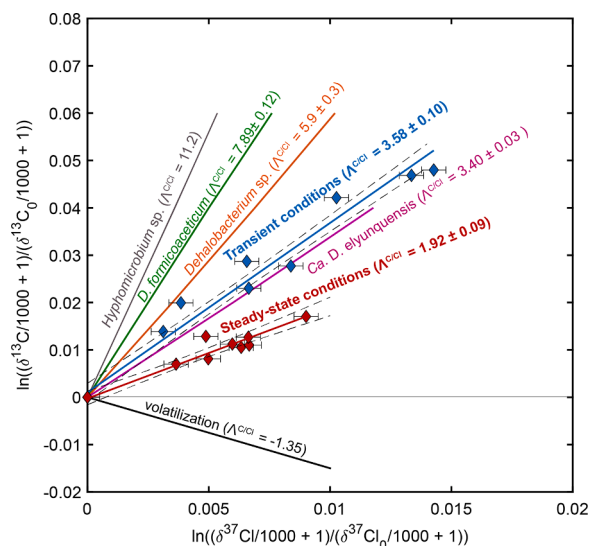


Fig. 3. Dual plot of $\Delta^{13}\text{C}$ versus $\Delta^{37}\text{Cl}$ for the degradation of DCM under steady-state (red squares) and transient (blue diamonds) conditions. The continuous lines represent the linear regression to derive the $\Lambda^{\text{C/Cl}}$ values and dashed lines represent the 95% confidence interval (C.I.), according to the York method. Reported values for DCM degradation by *Hyphomicrobium* strain MC8b (Heraty et al., 1999), *Dehalobacterium formicoaceticum* and *Ca. D. elyunquensis* (Chen et al., 2018), and *Dehalobacterium* sp. (Blázquez-Pallí et al., 2019) were added for comparison. Black line represents 99% of DCM volatilization (Huang et al., 1999).

Still, this value likely also reflects anaerobic DCM degradation, given that so far higher $\Lambda^{C/Cl}$ values (8.1 to 11.2) are rather associated with aerobic DCM degradation pathways (Heraty et al., 1999; Torgonskaya et al., 2019) (SI, Section I).

To date, anaerobic DCM degradation by bacteria affiliated with the *Peptococcaceae* family has been examined using C-Cl CSIA. Two distinct anaerobic degradation pathways were reported for DCM fermentation by *Dehalobacterium formicoaceticum* ($\Lambda^{C/Cl} = 7.89 \pm 0.12$) and DCM mineralization by *Ca. Dichloromethanomonas elyunquensis* ($\Lambda^{C/Cl} = 3.40 \pm 0.03$), and proposed to be associated with the Wood-Ljungdahl pathway (WLP) (Chen et al., 2018, 2020; Kleindienst et al., 2019). In addition, Blázquez-Pallí et al. (2019) reported a distinct $\Lambda^{C/Cl}$ value (5.9 ± 0.3) for anaerobic DCM degradation by a *Dehalobacterium*-containing culture, differing from that associated with *Dehalobacterium formicoaceticum* ($\Lambda^{C/Cl}$ value = 7.89 ± 0.12), although the two strains belong to the same genus. Different characteristics of the bacterial cell envelope or enzyme locations may result in distinct C and Cl isotope fractionation (Trueba-Santiso et al., 2017).

The differences in $\Lambda^{C/Cl}$ values under steady-state and transient conditions may thus reflect distinct C-Cl bond cleavage reactions and distinct anaerobic DCM degradation pathways. Further, our findings suggest that the prevalence of a given pathway depend on hydrochemical and hydrogeological dynamics in aquifers. Nevertheless, both laboratory aquifers likely feature a variety of DCM-degrading microorganisms, with the possibility of simultaneous operations of several different aerobic and anaerobic degradation pathways (Van Breukelen, 2007). In particular, the slight increase in O_2 levels in the fluctuation zone under transient conditions may be indicative of micro-oxic environments (SI, Sections E and F). However, the $\Lambda^{C/Cl}$ values obtained in our aquifers rather suggest the dominance of different anaerobic DCM degradation pathways, which is further supported by the presence of taxa associated to anoxic conditions (see below).

3.4. Water table fluctuations affect bacterial community composition and distribution of DCM-associated taxa

In total, 3,649,087 high-quality sequences were obtained, from which 69% and 31% corresponded to pore water (n=56) and sand samples (n=24), respectively. Rarefaction curves of diversity indices reached asymptotes with increasing sequencing depth, indicating sufficient sequencing efforts to capture the biodiversity extent of bacterial communities in both pore water and sand samples (SI, Section J).

Changes in bacterial diversity were analyzed using NMDS ordination

of relative OTU abundance. Diversity in sand samples (day 88) varied mainly as a function of O_2 gradients in the SZ and UZ (Fig. 4b). In contrast, differences in bacterial diversity in pore water samples (day 0-80) between inlet and outlet reservoirs suggested bacterial adaptation to DCM contamination along the flow path (Fig. 4a). Nevertheless, similar bacterial diversity under transient and steady-state conditions for both pore water and sand samples suggested that water table fluctuations did not play a major role in shaping the overall composition of bacterial communities (SI, Sections K and L).

Dominant taxa in aquifers may be associated with pollutants degradation pathways. In both aquifers, *Firmicutes* was the most abundant phylum in sand samples with up to 60% of retrieved sequences at lower depths (z = 15 cm, SI, Section L). Previous studies have shown the presence of this phylum in aquifers highly contaminated with VOCs (Hellal et al., 2021; Wright et al., 2017). Moreover, *Firmicutes* bacteria are known to utilize DCM as a sole carbon source under anoxic conditions (Kleindienst et al., 2017). Hence, the occurrence of *Firmicutes* supports the prevalence of anaerobic DCM biodegradation in both aquifers.

In pore water samples, the dominant OTU was associated with *Desulfosporosinus* under both steady-state and transient conditions (Fig. 5). Under steady-state conditions, *Desulfosporosinus* and *Geobacter* represented on average 25% and 12% of obtained sequences in the SZ, respectively, while *Dehalobacterium* and *Dehalococcoides* represented each approximately 10% (Fig. 5). Under transient conditions, in contrast, *Desulfosporosinus* increased from 25% to 58% relative abundance between days 0 and 13 in the SZ (z = 15 cm), corresponding to the first water table fluctuation event (Fig. 5). *Geobacter* was the second most abundant genus in the SZ representing up to 15% followed by *Dehalobacterium* (4%).

Co-occurrence of *Desulfosporosinus*, *Geobacter*, *Sulfurospirillum* and *Dehalococcoides* was reported previously in aquifers contaminated with halogenated contaminants (Hellal et al., 2021; Wright et al., 2017). This parallel enrichment of different OTUs without demonstrated association with DCM degradation suggest interspecies interactions in our laboratory aquifers. Such interactions could be indicative of concomitant degradation of DCM and other halogenated contaminants, as shown recently in investigations of other contaminated sites (Hellal et al., 2021; Trueba-Santiso et al., 2020; Blázquez-Pallí et al., 2019; Hermon et al., 2018; Wright et al., 2017). Detection of bacterial genera associated with OHR such as *Dehalococcoides* further supports the concomitant degradation of DCM and *cis*-DCE in our laboratory aquifers. Furthermore, reductive dechlorination of chlorinated ethenes such as *cis*-DCE relies on

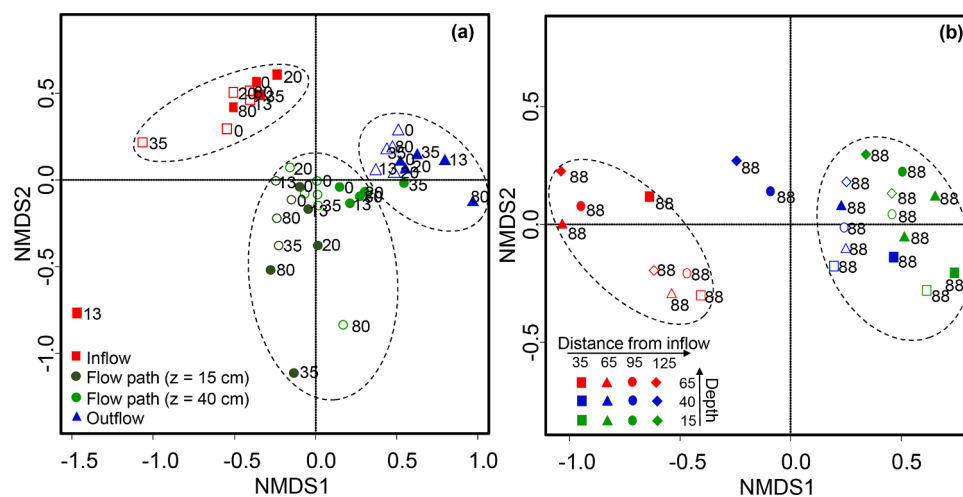


Fig. 4. NMDS ordination plot of bacterial diversity profiles from (a) pore water and (b) sand samples. Full symbols: transient conditions, empty symbols: steady-state conditions. Numbers next to symbols represent sampling day at 0, 13, 20, 35 and 80 for pore water samples and at day 88 for sand samples. Plot stress: (a) 0.11% and (b) 0.06%.

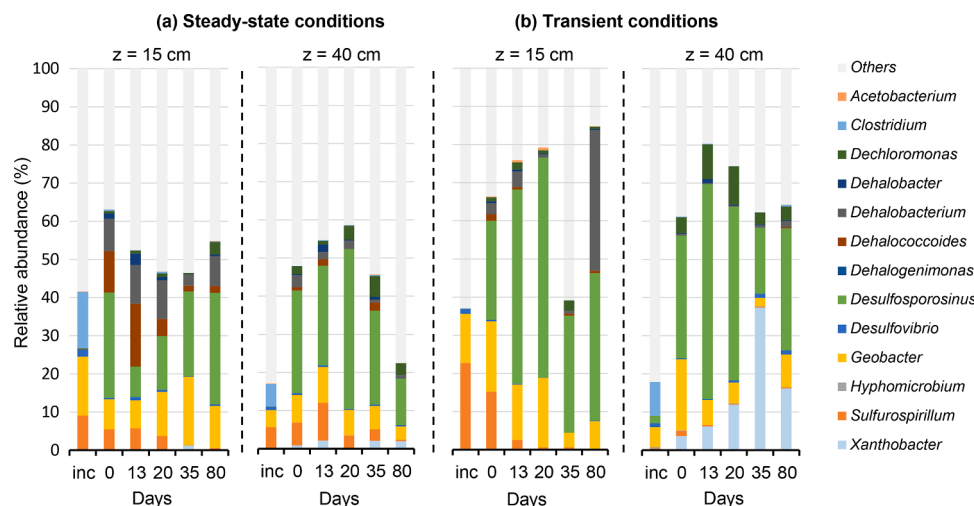


Fig. 5. Relative abundance of taxa associated with DCM degradation and OHR in lab-scale aquifers under (a) steady-state and (b) transient conditions in the saturated zone ($z = 15$ cm) and capillary fringe ($z = 40$ cm), and over time (from 0 to 80 days). Data includes the initial incubation period of 70 days (“inc” represents sampling 35 days prior to the experiments). Relative abundance (%) were normalized to the total sequence abundance for all defined OTUs.

H_2 as electron donor (DiStefano et al., 1992). Recently, it was proposed that DCM mineralization by *Ca. D. elyunquensis* produces H_2 and CO_2 (Chen et al., 2020), which may sustain reductive dechlorination in mixed contaminant plumes. Notably, for growth with DCM, *Ca. D. elyunquensis* requires the presence of H_2 -consuming partner populations performing H_2/CO_2 reductive acetogenesis, while *Dehalobacterium formicoaceticum* showed a strong dependence on CO_2 (Chen et al., 2020). Concomitant degradation of DCM and chlorinated ethenes in contaminated aquifers may thus result from interspecies metabolic networks associated with dehalogenative metabolism.

More generally, dynamic environmental conditions such as water table fluctuations can increase microbial metabolic activity (Pronk et al., 2020). Thus, we hypothesized that in the present study, water table fluctuations promoted a larger enrichment of *Desulfosporosinus* compared to steady-state conditions (Fig. 5). Kleindienst et al., 2019 reported that *Ca. D. elyunquensis* expressed similar WLP-associated enzymes as those of *Dehalobacter* and *Desulfosporosinus* spp. Hence, the similar C and Cl isotope fractionation determined here for DCM biodegradation under transient conditions ($\Delta^{C/Cl} = 3.58 \pm 0.42$) and by *Ca. Dichloromethanomonas elyunquensis* ($\Delta^{C/Cl} = 3.40 \pm 0.03$) (Chen et al., 2018) suggest that strains of the *Desulfosporosinus* genus may be DCM-degrading, in line with a previous report (Wright et al., 2017).

In contrast, the higher abundance of *Dehalobacterium* under steady-state conditions, and similar C fractionation values to those of a *Dehalobacterium*-containing culture (Blázquez-Pallí et al., 2019), suggest the occurrence of a fermentative DCM metabolism by as yet unknown *Dehalobacterium* strains ($\Delta^{C/Cl} = 1.92 \pm 0.30$). Worthy of note, a recent study proposed *Ca. Formimonas warabiya* strain DCMF as a novel DCM-fermenting bacterium of the *Peptococcaceae* family, capable of metabolizing DCM to acetate via the WLP (Holland et al., 2021) (SI, Section I). Clearly, bacteria associated with the *Peptococcaceae* family may play an important role in DCM biodegradation at contaminated sites.

4. Conclusions

Our study examined the effect of dynamic environmental conditions such as water table fluctuations on (i) hydrochemical conditions, (ii) bacterial responses, and in turn, (iii) on DCM degradation pathways in multi-contaminated aquifers. Our integrative approach combining C-Cl CSIA and biomolecular analyses suggested the prevalence of two distinct, possibly co-occurring, anaerobic DCM degradation pathways under steady-state and transient conditions. Bacterial diversity and

distribution of DCM-associated taxa was similar under both conditions. However, responses to water table fluctuations resulted in different bacterial community composition dominated by bacteria from the *Peptococcaceae* family, in particular *Desulfosporosinus* sp. We showed that environmental dynamics, which are often excluded from laboratory degradation experiments, can affect *in situ* DCM transformation. While current knowledge of anaerobic transformation pathways of DCM limits interpretation of DCM *in situ* biodegradation, fundamental research considering dynamics of environmental conditions are needed to improve bioremediation approaches at DCM contaminated sites in the future.

CRedit authorship contribution statement

Maria Prieto-Espinoza: Investigation, Methodology, Data curation, Visualization, Formal analysis, Writing – original draft, Writing – review & editing. **Sylvain Weill:** Conceptualization, Writing – review & editing. **Benjamin Belfort:** Investigation, Methodology, Writing – review & editing. **Emilie E.L. Muller:** Investigation, Writing – review & editing. **Jérémy Masbou:** Methodology, Formal analysis, Writing – review & editing. **François Lehmann:** Methodology, Writing – review & editing. **Stéphane Vuilleumier:** Conceptualization, Writing – review & editing. **Gwenaél Imfeld:** Conceptualization, Formal analysis, Funding acquisition, Project administration, Resources, Supervision, Writing – review & editing.

Declaration of Competing Interest

The authors declare that they have no known competing financial interests or personal relationships that could have appeared to influence the work reported in this paper.

Acknowledgments

This research was funded by the EC2CO-BIOHEFFECT program (CNRS-INSU) through the 2D-DCM project attributed to G.I. M.P.E. was supported by a fellowship of the Ecole Nationale du Génie de l’Eau et de l’environnement (ENGEES, France) and the doctoral school Earth and Environmental Sciences (ED 413) of University of Strasbourg. The authors acknowledge Dr. Jennifer Hellal for providing access to the Thémoril site, and to Dr. Charline Wiegert for help in mounting the laboratory aquifers and preliminary surveys. We thank Dr. Jordi Palau for measurements of chlorine standards. We are grateful to Benoît

Guyot, and Colin Fourtet, for technical assistance in the laboratory, Carmen Lázaro Sánchez for DNA extractions, and Dr. Tetyana Gylevska for fruitful discussions.

Associated content

Supplementary data related to this article can be found at xxxxx.

Supplementary materials

Supplementary material associated with this article can be found, in the online version, at [doi:10.1016/j.watres.2021.117530](https://doi.org/10.1016/j.watres.2021.117530).

References

- ATSDR, 2019. Substance Priority List. Retrieved: February 23, 2021 from <https://www.atsdr.cdc.gov/spl/index.html>.
- Blázquez-Pallí, N., Shouakar-Stash, O., Palau, J., Trueba-Santiso, A., Varias, J., Bosch, M., Soler, A., Vicent, T., Marco-Urrea, E., Rosell, M., 2019. Use of dual element isotope analysis and microcosm studies to determine the origin and potential anaerobic biodegradation of dichloromethane in two multi-contaminated aquifers. *Sci. Total Environ.* 696, 134066 <https://doi.org/10.1016/j.scitotenv.2019.134066>.
- Chen, G., Fisch, A.R., Gibson, C.M., Erin Mack, E., Seger, E.S., Campagna, S.R., Löffler, F. E., 2020. Mineralization versus fermentation: evidence for two distinct anaerobic bacterial degradation pathways for dichloromethane. *ISME J.* 14, 959–970. <https://doi.org/10.1038/s41396-019-0579-5>.
- Chen, G., Shouakar-Stash, O., Phillips, E., Justicia-Leon, S.D., Gilevska, T., Sherwood Lollar, B., Mack, E.E., Seger, E.S., Löffler, F.E., 2018. Dual carbon–chlorine isotope analysis indicates distinct anaerobic dichloromethane degradation pathways in two members of *Peptococcaceae*. *Environ. Sci. Technol.* 52, 8607–8616. <https://doi.org/10.1021/acs.est.8b01583>.
- Coplen, T.B., Brand, W.A., Gehre, M., Gröning, M., Meijer, H.A.J., Toman, B., Verkouteren, R.M., 2006. New guidelines for $\delta^{13}\text{C}$ measurements. *Anal. Chem.* 78, 2439–2441. <https://doi.org/10.1021/ac052027c>.
- DiStefano, T.D., Gossett, J.M., Zinder, S.H., 1992. Hydrogen as an electron donor for dechlorination of tetrachloroethene by an anaerobic mixed culture. *Appl. Environ. Microbiol.* 58, 3622–3629. <https://doi.org/10.1128/AEM.58.11.3622-3629.1992>.
- Elsner, M., 2010. Stable isotope fractionation to investigate natural transformation mechanisms of organic contaminants: principles, prospects and limitations. *J. Environ. Monit.* 12, 2005–2031. <https://doi.org/10.1039/C0EM00277A>.
- Elsner, M., Imfeld, G., 2016. Compound-specific isotope analysis (CSIA) of micropollutants in the environment — current developments and future challenges. *Curr. Opin. Biotechnol.* 41, 60–72. <https://doi.org/10.1016/j.copbio.2016.04.014>.
- Elsner, M., McKelvie, J., Lacrampe Couloume, G., Sherwood Lollar, B., 2007. Insight into methyl tert-butyl ether (MTBE) stable isotope fractionation from abiotic reference experiments. *Environ. Sci. Technol.* 41, 5693–5700. <https://doi.org/10.1021/es070531o>.
- EPA, 2020. Risk Evaluation for Methylene Chloride (dichloromethane, DCM). U.S. Environmental Protection Agency, Washington, D.C. EPA-740-R1-8010.
- European Commission. (2013). Priority substances and certain other pollutants according to Annex II of Directive 2008/105/EC - Environment - European Commission. https://ec.europa.eu/environment/water/water-framework/priority_substances.htm.
- Fischer, A., Manefield, M., Bombach, P., 2016. Application of stable isotope tools for evaluating natural and stimulated biodegradation of organic pollutants in field studies. *Curr. Opin. Biotechnol.* 41, 99–107. <https://doi.org/10.1016/j.copbio.2016.04.026>.
- Gossett, J.M., 1987. Measurement of Henry's law constants for C1 and C2 chlorinated hydrocarbons. *Environ. Sci. Technol.* 21, 202–208. <https://doi.org/10.1021/es00156a012>.
- Haberer, C.M., Rolle, M., Cirkpa, O.A., Grathwohl, P., 2012. Oxygen transfer in a fluctuating capillary fringe. *Vadose Zone J.* 11 <https://doi.org/10.2136/vzj2011.0056>.
- Heckel, B., Rodríguez-Fernández, D., Torrentó, C., Meyer, A., Palau, J., Domènech, C., Rosell, M., Soler, A., Hunkeler, D., Elsner, M., 2017. Compound-specific chlorine isotope analysis of tetrachloromethane and trichloromethane by gas chromatography-isotope ratio mass spectrometry vs gas chromatography-quadrupole mass spectrometry: method development and evaluation of precision and trueness. *Anal. Chem.* 89, 3411–3420. <https://doi.org/10.1021/acs.analchem.6b04129>.
- Hellal, J., Joulian, C., Urien, C., Ferreira, S., Denonfoux, J., Hermon, L., Vuilleumier, S., Imfeld, G., 2021. Chlorinated ethene biodegradation and associated bacterial taxa in multi-polluted groundwater: Insights from biomolecular markers and stable isotope analysis. *Sci. Total Environ.* 763, 142950 <https://doi.org/10.1016/j.scitotenv.2020.142950>.
- Heraty, L.J., Fuller, M.E., Huang, L., Abrajano, T., Sturchio, N.C., 1999. Isotopic fractionation of carbon and chlorine by microbial degradation of dichloromethane. *Org. Geochem.* 30, 793–799. [https://doi.org/10.1016/S0146-6380\(99\)00062-5](https://doi.org/10.1016/S0146-6380(99)00062-5).
- Hermon, L., Denonfoux, J., Hellal, J., Joulian, C., Ferreira, S., Vuilleumier, S., Imfeld, G., 2018. Dichloromethane biodegradation in multi-contaminated groundwater: insights from biomolecular and compound-specific isotope analyses. *Water Res.* 142, 217–226. <https://doi.org/10.1016/j.watres.2018.05.057>.
- Höhener, P., Imfeld, G., 2021. Quantification of Lambda (Λ) in multi-elemental compound-specific isotope analysis. *Chemosphere* 267, 129232. <https://doi.org/10.1016/j.chemosphere.2020.129232>.
- Holland, S.L., Ertan, H., Montgomery, K., Manefield, M.J., Lee, M., 2021. Novel dichloromethane-fermenting bacteria in the *Peptococcaceae* family. *ISME J.* 15, 1709–1721. <https://doi.org/10.1038/s41396-020-00881-y>.
- Holt, B.D., Sturchio, N.C., Abrajano, T.A., Heraty, L.J., 1997. Conversion of chlorinated volatile organic compounds to carbon dioxide and methyl chloride for isotopic analysis of carbon and chlorine. *Anal. Chem.* 69, 2727–2733. <https://doi.org/10.1021/ac961096b>.
- Huang, L., Sturchio, N.C., Abrajano, T., Heraty, L.J., Holt, B.D., 1999. Carbon and chlorine isotope fractionation of chlorinated aliphatic hydrocarbons by evaporation. *Org. Geochem.* 30, 777–785. [https://doi.org/10.1016/S0146-6380\(99\)00060-1](https://doi.org/10.1016/S0146-6380(99)00060-1).
- Hunkeler, D., Aravena, R., Berry-Spark, K., Cox, E., 2005. Assessment of degradation pathways in an aquifer with mixed chlorinated hydrocarbon contamination using stable isotope analysis. *Environ. Sci. Technol.* 39, 5975–5981. <https://doi.org/10.1021/es048464a>.
- Hunkeler, D., Meckenstock, R.U., Sherwood Lollar, B., 2009. A Guide for Assessing Biodegradation and Source Identification of Organic Ground Water Contaminants Using Compound Specific Isotope Analysis (CSIA). U.S. Environmental Protection Agency, Washington, D.C., p. 82. EPA/600/R-08/148.
- Jeannotat, S., Hunkeler, D., 2013. Can soil gas VOCs be related to groundwater plumes based on their isotope signature? *Environ. Sci. Technol.* 47, 12115–12122. <https://doi.org/10.1021/es4010703>.
- Jin, B., Laskov, C., Rolle, M., Haderlein, S.B., 2011. Chlorine isotope analysis of organic contaminants using GC-qMS: method optimization and comparison of different evaluation schemes. *Environ. Sci. Technol.* 45, 5279–5286. <https://doi.org/10.1021/es200749d>.
- Kaufmann, R., Long, A., Bentley, H., Davis, S., 1984. Natural chlorine isotope variations. *Nature* 309, 338–340. <https://doi.org/10.1038/309338a0>.
- Kleindienst, S., Chourey, K., Chen, G., Murdoch, R.W., Higgins, S.A., Iyer, R., Campagna, S.R., Mack, E.E., Seger, E.S., Hettich, R.L., Löffler, F.E., 2019. Proteogenomics reveals novel reductive dehalogenases and methyltransferases expressed during anaerobic dichloromethane metabolism. *Appl. Environ. Microbiol.* 85 <https://doi.org/10.1128/AEM.02768-18>.
- Kleindienst, S., Higgins, S.A., Tsementzi, D., Chen, G., Konstantinidis, K.T., Mack, E.E., Löffler, F.E., 2017. '*Candidatus* Dichloromethanomonas elyunquensis' gen. nov., sp. nov., a dichloromethane-degrading anaerobe of the *Peptococcaceae* family. *Syst. Appl. Microbiol.* 40, 150–159. <https://doi.org/10.1016/j.syapm.2016.12.001>.
- Lee, M., Wells, E., Wong, Y.K., Koenig, J., Adrian, L., Richnow, H.H., Manefield, M., 2015. Relative contributions of *Dehalobacter* and zerovalent iron in the degradation of chlorinated methanes. *Environ. Sci. Technol.* 49, 4481–4489. <https://doi.org/10.1021/es5052364>.
- McCarthy, K.A., Johnson, R.L., 1993. Transport of volatile organic compounds across the capillary fringe. *Water Resour. Res.* 29, 1675–1683. <https://doi.org/10.1029/93WR00098>.
- NRC, 1993. In Situ Bioremediation: When Does it Work? The National Academies Press, Washington, DC. <https://doi.org/10.17226/2131>.
- Ojeda, A.S., Phillips, E., Sherwood Lollar, B., 2020. Multi-element (C, H, Cl, Br) stable isotope fractionation as a tool to investigate transformation processes for halogenated hydrocarbons. *Environ. Sci.* 22, 567–582. <https://doi.org/10.1039/c9em00498j>.
- Peralta, A.L., Ludmer, S., Matthews, J.W., Kent, A.D., 2014. Bacterial community response to changes in soil redox potential along a moisture gradient in restored wetlands. *Ecol. Eng.* 73, 246–253. <https://doi.org/10.1016/j.ecoleng.2014.09.047>.
- Pope, D., Hurt, K., Wilson, B., Acree, S., Levine, H., Mangion, S., 2004. Performance Monitoring of MNA Remedies for VOCs in Ground Water. U.S. Environmental Protection Agency, Washington, D.C. p. 92. EPA/600/R-04/027.
- Pronk, G.J., Mellage, A., Milojevic, T., Smeaton, C.M., Engel, K., Neufeld, J.D., Rezanezhad, F., Cappellen, P.V., 2020. Carbon turnover and microbial activity in an artificial soil under imposed cyclic drainage and imbibition. *Vadose Zone J.* 19, e20021. <https://doi.org/10.1002/vzj2.20021>.
- Core Team, R., 2019. R: A Language and Environment for Statistical Computing, Version 3.5.3. R Foundation for Statistical Computing. <https://www.R-project.org/>.
- Rühle, F.A., von Netzer, F., Lueders, T., Stumpp, C., 2015. Response of transport parameters and sediment microbiota to water table fluctuations in laboratory columns. *Vadose Zone J.* 14, 12. <https://doi.org/10.2136/vzj2014.09.0116>.
- Schlosser, P.M., Bale, A.S., Gibbons, C.F., Wilkins, A., Cooper, G.S., 2015. Human health effects of dichloromethane: key findings and scientific issues. *Environ. Health Perspect.* 123, 114–119. <https://doi.org/10.1289/ehp.1308030>.
- Schürner, H.K.V., Maier, M.P., Eckert, D., Brejcha, R., Neumann, C.-C., Stumpp, C., Cirkpa, O.A., Elsner, M., 2016. Compound-specific stable isotope fractionation of pesticides and pharmaceuticals in a mesoscale aquifer model. *Environ. Sci. Technol.* 50, 5729–5739. <https://doi.org/10.1021/acs.est.5b03828>.
- Seybold, C.A., Mersie, W., Huang, J., McNamee, C., 2002. Soil redox, pH, temperature, and water-table patterns of a freshwater tidal wetland. *Wetlands* 22, 149–158. [https://doi.org/10.1672/0277-5212\(2002\)022\[0149:SRPTAW\]2.0.CO;2](https://doi.org/10.1672/0277-5212(2002)022[0149:SRPTAW]2.0.CO;2).
- Shestakova, M., Sillanpää, M., 2013. Removal of dichloromethane from ground and wastewater: a review. *Chemosphere* 93, 1258–1267. <https://doi.org/10.1016/j.chemosphere.2013.07.022>.
- Smets, B.F., Pritchard, P., 2003. Elucidating the microbial component of natural attenuation. *Curr. Opin. Biotechnol.* 14, 283–288. [https://doi.org/10.1016/S0958-1669\(03\)00062-4](https://doi.org/10.1016/S0958-1669(03)00062-4).

- Tamura, H., Goto, K., Yotsuyanagi, T., Nagamaya, M., 1974. Spectrophotometric determination of iron(II) with 1,10-phenanthroline in the presence of large amounts of iron(III). *Talanta* 21, 314–318. [https://doi.org/10.1016/0039-9140\(74\)80012-3](https://doi.org/10.1016/0039-9140(74)80012-3).
- Thullner, M., Centler, F., Richnow, H.-H., Fischer, A., 2012. Quantification of organic pollutant degradation in contaminated aquifers using compound specific stable isotope analysis – Review of recent developments. *Org. Geochem.* 42, 1440–1460. <https://doi.org/10.1016/j.orggeochem.2011.10.011>.
- Torgonskaya, M.L., Zyakun, A.M., Trotsenko, Y.A., Laurinavichius, K.S., Kümmel, S., Vuilleumier, S., Richnow, H.H., 2019. Individual stages of bacterial dichloromethane degradation mapped by carbon and chlorine stable isotope analysis. *J. Environ. Sci.* 78, 147–160. <https://doi.org/10.1016/j.jes.2018.09.008>.
- Trueba-Santiso, A., Fernández-Verdejo, D., Marco-Rius, I., Soder-Walz, J.M., Casabella, O., Vicent, T., Marco-Urrea, E., 2020. Interspecies interaction and effect of co-contaminants in an anaerobic dichloromethane-degrading culture. *Chemosphere* 240, 124877. <https://doi.org/10.1016/j.chemosphere.2019.124877>.
- Trueba-Santiso, A., Parladé, E., Rosell, M., Lliros, M., Mortan, S.H., Martínez-Alonso, M., Gaju, N., Martín-González, L., Vicent, T., Marco-Urrea, E., 2017. Molecular and carbon isotopic characterization of an anaerobic stable enrichment culture containing *Dehalobacterium* sp. during dichloromethane fermentation. *Sci. Total Environ.* 640–648. <https://doi.org/10.1016/j.scitotenv.2016.12.174>, 581–582.
- Van Breukelen, B.M., 2007. Extending the Rayleigh equation to allow competing isotope fractionating pathways to improve quantification of biodegradation. *Environ. Sci. Technol.* 41, 4004–4010. <https://doi.org/10.1021/es0628452>.
- Vermeesch, P., 2018. IsoplotR: a free and open toolbox for geochronology. *Geosci. Front.* 9, 1479–1493. <https://doi.org/10.1016/j.gsf.2018.04.001>.
- Williams, M.D., Ostrom, M., 2000. Oxygenation of anoxic water in a fluctuating water table system: An experimental and numerical study. *J. Hydrol.* 230, 70–85. [https://doi.org/10.1016/S0022-1694\(00\)00172-4](https://doi.org/10.1016/S0022-1694(00)00172-4).
- Wright, J., Kirchner, V., Bernard, W., Ulrich, N., McLimans, C., Campa, M.F., Hazen, T., Macbeth, T., Marabello, D., McDermott, J., Mackelprang, R., Roth, K., Lamendella, R., 2017. Bacterial community dynamics in dichloromethane-contaminated groundwater undergoing natural attenuation. *Front. Microbiol.* 8, 2300. <https://doi.org/10.3389/fmicb.2017.02300>.
- Zhang, Z., Furman, A., 2021. Soil redox dynamics under dynamic hydrologic regimes -A review. *Sci. Total Environ.* 763, 143026 <https://doi.org/10.1016/j.scitotenv.2020.143026>.